© 2018 IJSRSET | Volume 4 | Issue 10 | Print ISSN: 2395-1990 | Online ISSN : 2394-4099
Themed Section : Engineering and Technology

Adaptive Genetic Algorithm Based Three Dimensional Positioning (AgaTdp) for Radio Frequency Identification Networks

R. Maruthaveni[1], Dr. V. Kathiresn[2]
[1]Assistant. Professor, Coimbatore,Tamil Nadu, India
[2]COE, Coimbatore, Tamil Nadu, India

ABSTRACT

There exists vast research works to be carried out in Visible Light Communication (VLC) indoor 3D positioning. This happened due to lessening features from various Light Emitting Diodes (LEDs), the three-dimensional directions of the receiver possibly will perform constraint equations. In certain areas of VLC positioning system, positioning precision is constrained due to the system noise and non-perfect gadgets. Hence, an adaptive GA is employed to subtle the positioning errors that facilitate 3D of the receiver. Positioning directions are controlled by evaluatedas indicated by the principle of trilateration. Performance metrics such as reality value versus predictive value, error rate, convergence speed and accuracy are taken into account for comparing the proposed work with the existing work PSO-BP. Results demonstrated that the proposed AGA-TDP performs better than that of PSO-BP.

Keywords : Networks, Wireless, RFID, Localization, Received Signal Strength, Accuracy, Optimization.

I. INTRODUCTION

With the fast progression of wireless sensor technology, versatile technology and Internet technology, the enthusiasm for arranging and course is twisting up progressively well known. In any case, it is essential to know the authentic location of articles in various indoor scenes, for instance, the location of stock in broad circulation focuses, following the circumstance of rigging at the air terminal and steady achieving the circumstance of the prisoners in a splendid correctional facility and so on. In this way, Indoor localization technique has caused expansive concern. The ordinary RFID arranging system in light of RSSI is most fundamental to choose the indoor way misfortune model of RSSI-DIST, paying little mind to whether the dissent is stationary or moving [1]. By then the circumstance of target is figured by some position isolate figuring's. Regardless, this strategy is unnecessarily dependent on experience show. Additionally, in view of alterable and multi-path transmission in the genuine indoor condition requires the parameters of model changed dependably. In this way, it is outstandingly difficult to develop the correct flag misfortune show in the indoor localization structure. To handle the previously mentioned challenges, we first need to empower the RSSI motion from detached labels to screen the entire observation region in an effective and subtle way. In this manner we send an arrangement of detached RFID labels and peruses (with receivingantenna) to frame a RSS field that can cover the entire checked region.

II. RELATED WORKS

With the dangerously expanding maturing populace, shrewd space that can better help the autonomous living of the elderly has been drawing in the

expanding consideration both from industry and the scholarly world. One of the key preconditions for such a savvy domain lies on a precise and auspicious identification of clients' areas and day by day schedules [1, 2], particularly for an indoor situation that GPS (Global Position System) can't deal with [3]. To handle this test, an extensive variety of indoor localization and following systems have been proposed throughout the previous two decades, including however not restricted to LANDMARC [4], WILL [5], Tagoram [6] and BackPos [7]. However the greater part of the methodologies are wearable-gadget based strategy that unavoidably requires the client to effectively convey at least one gadgets, for example, different sorts of sensors, advanced cells, RFID labels/per-users or other Radio Frequency (RF) handsets, in this manner raising numerous natural unrealistic issues as a general rule [8]. For instance, the connected sensors/labels might be harmed or lost. It is likewise obstructive and awkward for the client to wear gadgets constantly, particularly considering that numerous electronic gadgets have a direct size or weight. For this end, gadget free (additionally called inconspicuous) detached indoor localization has increased more consideration of late and numerous promising methodologies have been proposed [9, 10, 11, 12]. One well known gadget free human following method is based upon the current progress of PC vision, which creates different models to catch human development from pictures or recordings by utilizing RGB cameras [13, 14], or infrared sensors [15] or profundity cameras (e.g., Kinect) [16]. However PC vision based methodologies require the followed client inside the viewable pathway of a camera, and more often than not neglect to work in a darkened situation [13]. In addition, vision-based strategy can likewise be thought to be protection obtrusive [1]. Another DfP localization method is to seriously misuse the radio-frequency flag, e.g., restricting the objective by examining the Received Signal Strength (RSS) varieties [17, 18, 2] or Channel State Information (CSI) [19, 20] in WIFI, or following the client through a divider by translating the radio waves reflected of human development [21]. In spite of the fact that promising, these systems frequently require specific RF flags, for example, Frequency-Modulated Continuous Wave (FMCW) or expand upon exorbitant unique reason gadgets, for example, USRP (all inclusive programming radio fringe), or need to alter the low-level firmware, for example, abstracting CSI signals. In particular, they all require general upkeep, for example, battery substitution, along these lines thwarting their down to earth arrangement in reality [1, 8]. Particle Swarm Optimization (PSO)-based Back Propagation (BP) neural network (PSO-BP) [22] was used to determine the relationship between the RFID signals and the position of a tag for an RFID-based positioning system.

III. ADAPTIVE GENETIC ALGORITHM BASED THREE DIMENSIONAL POSITIONING (AGATDP)

3.1. The Channel Model of Indoor Optical Communication

In the indoor positioning system in light of clear light communication, light sources (LEDs) are viewed as reference focuses, and the terminal is the optical flag receiver. The positioning system comprises of two sections: (1) LEDs installed on the roof of the room model. (2) The receiver. With a specific end goal to portray the indoor optical communication process, a few parameters are presented. The separation amongst LEDs and the receiver are characterized as d, the edge of irradiance as for the opposite rotate of the transmitter is characterized as θ, the frequency edge as for the receiver's ordinary is characterized as ϕ and the introduction point between the receivers typical and the vertical is characterized as φ.

LEDs can be compact with as Lambertian sources for their substantial beam variation when talked about in the indoor positioning. The channel pick up of a line-of-sight (LOS) remote channel can be portrayed by the accompanying Formula [19]:

$$H(0) = \begin{cases} \frac{m_t + 1}{2\pi d^2} AT_S(\phi) G(\phi) cos^{m_t}(\theta) cos^{m_r}(\phi), & 0 \le \phi \le \Psi_c \\ 0 \ , \phi \ge \Psi_c \end{cases} \quad (1)$$

where the workable area of PD is given by the consistent A, the channel pick up and concentrator pick up are given by T_S $(\phi)$and $G(\phi)$, and the FOV of PD is characterized as Ψ_c. The Lambertian parameters can be spoken to as takes after:

$$\begin{cases} m_t = -\frac{In2}{In(cos\theta_{1/2}} \\ m_r = -\frac{In2}{In(cos\phi_{1/2}} \end{cases} \quad (2)$$

where $\theta_{1/2}$and $\phi_{1/2}$ are the half-control points of the transmitter (LED) and the receiver (PD) separately. $\theta_{1/2}$ refers to the point at which luminous power is half of the hub (typical) luminous force and $\phi_{1/2}$ refers to the edge at which got flag quality (photocurrent reaction) is half of the incentive in the ordinary course. Gotten optical power P_r can be spoken to as:

$$P_r = P_t H(0) + P_{background} \quad (3)$$

where P_t is the normal transmitted optical power, and $P_{background}$ is the event optical power caused by other optical resources existing out of sight condition. Go above and beyond, we may utilize the methods for normal electric current μI_r to quantify the event optical power delivered by the PD:

$$\mu I_r = \frac{R_p P_r}{A} \quad (4)$$

where R_p is the responsivity of the PD, it is steady to the optical flag with a similar wavelength. [18] The normal PD current is partial by two noise forms: (1) shot disorder which is caused by event optical power including the popular flag and lighting condition. (2) the thermal noise which is caused by the stochastic conduct of electrons. The aggregate noise σ^2_{noise}can have appeared as a Gauss procedure which is the total of shot disorder σ^2_{shot} and thermal noise $\sigma^2_{thermal}$, spoke to as [21]:

$$\sigma^2_{noise} = \sigma^2_{shot} + \sigma^2_{thermal} \quad (5)$$

$$\sigma^2_{shot} = 2_q R_p P_r + 2_q I_{bg} I_2 B \quad (6)$$

$$\sigma^2_{thermal} = \frac{8\pi k T_k}{G_0} \eta A I_2 B^2 + \frac{16\pi^2 k \Gamma T_k}{g_m} \eta^2 A^2 I_3 B^2 \quad (7)$$

In these formulas, $, q, B, k, I_{bg}, T_k, G_0, \Gamma, \eta, g_m$ is the basic charge, comparative disorder bandwidth, the Boltzmann consistent, foundation present, supreme temperature, the open circle voltage pick up, the channel noise factor, the settled capacitance of photo-detector (PD), and the trans-conductance, separately. I_2 *and* I_3 are the disorders bandwidth factors.

3.2. Positioning Principle of RSS

RSS algorithm based VLC indoor positioning systems utilize get flag quality to appraise removes between the receiver and transmitters. Then the trilateration is utilized to decide the area. In the circumstance of 2D positioning, as a rule, circumstance, three LEDs are required in any event, because of the way that three drifts at any rate can converge at a certain point. Concerning 3D positioning, more than three LEDs are expected to wipe out the surplus arrangements. The hub model of VLC indoor positioning system can be represented as follows: in 3D space, there are m LED reference point hubs, the rest of the $n - m$ hubs are obscure hubs. By estimating the force decrease of the optical signs, the separation $d_{i,j}$ between guide hub i and obscure hub j can be resolved by the crossing point states of different circles.

Indicate $d_{i,j,xy}$ as evaluated level separations from the obscure hub j and reference point hub $i, d_{ij,xy}$ can be spoken to as:

$$d_{ij,xy}^2 = d_{i,j}^2 - (H - z_e)^2 \quad (8)$$

where H is the aggregate importance of the positioning unit, and $(H - z_e)$ is the vertical separation between the LED and the positioning terminal plane. The condition for trilateration in 3D positioning system can be express as the associated quadratic conditions:

$$\begin{cases} (x_e - x_1)^2 + (y_e - y_1)^2 = d_{1J,xy}^2 \\ (x_e - x_2)^2 + (y_e - y_2)^2 = d_{2J,xy}^2 \\ (x_e - x_3)^2 + (y_e - y_3)^2 = d_{3J,xy}^2 \\ (x_e - x_n)^2 + (y_e - y_n)^2 = d_{nJ,xy}^2 \end{cases} \quad (9)$$

where $[x_1, x_2, x_3, \dots, x_n]$ and $[y_1, y_2, y_3, \dots, y_n]$ are the $X\ and\ Y$ directions of signal hubs used in positioning system, $[d_{1,xy}, d_{2,xy}, d_{3,xy} \dots d_{n,xy}]$ are even separations from receiver to guide hubs and $[x_e y_e z_e]$ are directions of the obscure hub. The evaluated remove $d_{ij,xy}^2$can be gotten by estimating the power declining element of signal hub I and obscure node$j$ $H_{(j)}^{(i)}(0)$which can be express as:

$$H_{(j)}^{(i)}(0) = \frac{P_{r,j}}{P_{t,i}} \quad (10)$$

3.3. Positioning System Configuration

With a specific end goal to overcome the issue of shared impedance in flag resources, Code Division Multiple Access (CDMA) innovation is presented. As appeared in Figure 2, information that the transmitters communicate is handled in following advances:

(1) Each LED gets an ID code which is identified by its geographical position. $\overrightarrow{S_i}$ is utilized to speak to the ID code of the ith transmitter which is a double arrangement. $\overrightarrow{S_i}$ can be composed in the accompanying structure:

$$\overrightarrow{S_i} = S_{i,1}, S_{i,2}, \dots S_{i,n} \quad (11)$$

where n is number of the bits that an ID information code contains.

(2) Generate baseband flag utilizing on-off keying (OOK) modulation.

(3) Coordinate arrangement spreading range modulation. This progression contains two processes: distribution and scrambling: the flag is balanced by a spread range operation first and then scrambling code is stacked into the regulated flag. Here, m arrangement is utilized as the channel code while the Walsh code is utilized as the address code. Walsh code with a length of $2^n\ and\ 2^n$ components can be generated by the Hadamard network. The repeat relation of the Hadamard network can be communicated as follows:

$$H_n = \begin{pmatrix} H_{n-1} & H_{n-1} \\ H_{n-1} & H_{n-1} \end{pmatrix} \quad (12)$$

In the event that there are M LEDs in the system, an arrangement of PN code with a length of M is required. Expecting PN code successions with a length of M is $\vec{C_i} = \{C_{i,1}, C_{i,2}, \dots, C_{i,M}\}, i = 1, 2, \dots, M$ as indicated by the association of PN code, the arrangements ought to have the accompanying property [22]:

$$\langle \vec{C_i}. \vec{C_j} \rangle = \sum_{i=1}^{m} C_{i,k}^* C_{j,k} = \begin{cases} M, & i = j \\ o, & i \neq j \end{cases} \quad (13)$$

At the receiver, the blended optical flag can be spoken to by the accompanying Formula:

$$r_{n,k} = P_r \sum_{i=1}^{m} S_{i,n} C_{i,k} \quad (14)$$

where $S_{i,n}$ speaks to the nth information image of the ith LED and m represents the number of LEDs in the system. As indicated by Eq. (14), the yield of the jth versatile channel can be spoken to by the accompanying equation:

$$Y_{j,n} = \langle \vec{r}_{n,k}.\vec{C}_j \rangle = \sum_{k=1}^{M}(C_{j,k}P_r \sum_{i=1}^{m} S_{i,n}C_{i,k}) = P_r S_{i,n} \quad (15)$$

The last demodulation flag can be gotten by an integration of $Y_{j,n}$::

$$Y_j = \sum_{n=1}^{n=N} Y_{j,n} \quad (16)$$

3.4. Three-Dimensional Positioning Algorithm based on GA

In many works of VLC indoor 3D positioning, as indicated by the decrease factors from various LEDs, the three-dimensional directions of the receiver can be dictated by understanding the constraint equations. Be that as it may, in genuine application situations of the VLC positioning system, positioning precision is constrained due to the system noise and non-perfect gadgets. Keeping in mind the end goal to settle the positioning mistake, GA is proposed to calculate the 3D facilitate of the receiver. As the Formula (9) shows, positioning directions are controlled by evaluated removes amongst transmitters and the receiver. however, as indicated by the principle of trilateration, evaluated separations must fulfil the condition that all circles in Figure 3 communicate at a certain point. In other words, in spite of the fact that evaluated separations are influenced by different components, by changing charged separations to check that all circles cooperate at a certain point, positioning blunder can reduce. Here a few notations are made first: the deliberate $H(0)$ of the nth LED is characterized as $H^{(n)}(0)$, the separation between the nth LED is characterized as $d^{(n)}$.

In the system configuration, 4 LEDs are chosen to be a positioning unit and the proposed positioning algorithm based on GA can be portrayed as the accompanying advances.

3.4.1 Generate the Population

In this progression, the person of a population contains 11 chromosomes in which 3 chromosomes speak to the 3 diverse facilitate component (x, y, z) and the rest of the 8 chromosomes speak to the mistake correction parameter $\gamma_n \; and \; \epsilon_n$ $(n = 1, 2, 3, 4)$. Keeping in mind the end goal to streamline the last hybrid operation and mutation operation, the parallel encoding is utilized. In the double encoding of an individual, the length of chromosomes l decides calculation precision. Distinctive to traditional GA, keeping in mind the end goal to enhance population assorted variety, when an individual is generated, closeness check of the individual will be done. Characterize a closeness constant ζ to quantify the similitude of two people:

$$\zeta = \frac{l_{same}}{l} \quad (17)$$

In this Formula, l_{same} is a number of the similar qualities. A limit ζ_0 is set to judge whether the recently generated individual is like an individual existing in the population. In the event that ζ is higher than the edge ζ_0 , this individual ought to be generated again. After the generation of the population, a person of the population can be composed as the network frame $(X, Y , Z, \epsilon_1, \epsilon_2, \epsilon_3, \epsilon_4, \gamma_1, \gamma_2, \gamma_3, \gamma_4)$ where the every one of the components is Double section vectors with the chromosome length l. Consequently, a person in the algorithm can be express in the accompanying twofold framework shape:

$$(X, Y , Z, \epsilon_1, \epsilon_2, \epsilon_3, \epsilon_4, \gamma_1, \gamma_2, \gamma_3, \gamma_4) = \begin{pmatrix} X_1 & \cdots & \gamma_{4,1} \\ \vdots & \ddots & \vdots \\ X_1 & \cdots & \gamma_{4,1} \end{pmatrix} \quad (18)$$

It ought to be underlined that twofold coding is utilized specifically in GA to look and improve the parameters in a positioning system.

3.4.2 Calculate the Fitness

As per Eq. (3), in the event that we overlook the impact of the energy foundation light force, we can signify $P_r^{(n)}$ as the got flag control at the receiver:

$$P_r^{(n)} = H(0)P_t = \frac{m+1}{2\pi d^2} AT_S(\phi)G(\phi)cos^{m_r}(\phi)P_t \quad (19)$$

where n is the serial number of LEDs, P_t is the flag transmit optical power, and $\theta = cos^{-1}\left(\frac{h}{d}\right)$, h ,his the vertical separation between the transmitter and receiver. In a general situation, two Lambertian parameters m_t and m_r are utilized to portray light power distribution of LEDs and photocurrent response distribution of PD individually, which can be compact with as constants to fit directivity bend. And accept $m_t = m_r = 1$in simulation model and $C = \frac{m+1}{2\pi} AT_S(\phi)G(\phi)$is a constant initially to assess disagreeable separation. The Formula (19) can be rearranged to the accompanying structure:

$$P_r^{(n)} = \frac{C}{d^2}\cos(\theta)\cos(\phi)P_t \quad (20)$$

Furthermore, accepting the receiver is placed horizontally in order to update the examination, the radiation edge of PD ϕ and the radiation edge of LED θ is considered equivalent. And expect the energy of transmitters is same, the unpleasant separation $d^{(n)}$ between the LED n and the receiver can be spoken to as [4]:

$$d^{(n)} = \sqrt[4]{Ch^2\frac{P_t}{P_r^{(n)}}} = \sqrt[4]{Ch^2\frac{1}{H^{(n)}(0)}} \quad (21)$$

In any case, $d^{(n)}$ aren't exact evaluated separations, since system noise and the gain of optical channel and concentrator $T_s(\phi)G(\phi)$ aren't considered? Two assumptions are made earlier: (1) disorder control is much lower than flag control. Consequently, estimating mistake caused by disorder is generally little contrasted and the estimation of $H^{(n)}(0)$ itself. (2) Lambertian parameters portray unkind response bend of PD, in neighbourhood occurrence edge, because of optical focal point and dispersivity of gadget execution, the response will go wrong from the condition equation (21). With a specific end goal to acquire exact separation, ϵ_n is used to reward estimating deviation caused by system noise and $\gamma_n$is used to repay estimating deviation caused by a response-fitting mistake of PD. The altered separation $d_c^{(n)}$ can be communicated as:

$$d_c^{(n)} = \sqrt[4]{Ch^2\frac{1}{\gamma_n H^{(n)}(0) \pm \epsilon_n}} \quad (22)$$

Formula (18) demonstrates an individual spoke to in double grid shape. On the off chance that the maximum spatial scope of room model is characterized as (*L*,,), by binary-to-decimal conversion, decimal space arrange (x_0, y_0, z_o) of the individual can be spoken to as the accompanying Formula:

$$\begin{cases} x_0 = \frac{L\sum_{i=1}^{l} X_i 2^{i-1}}{2^l - 1} \\ y_0 = \frac{W\sum_{i=1}^{l} X_i 2^{i-1}}{2^l - 1} \\ z_0 = \frac{H\sum_{i=1}^{l} X_i 2^{i-1}}{2^l - 1} \end{cases} \quad (23)$$

where l is the chromosome length.

Accept space directions of the 4 transmitters are $(x_{L_n}, y_{L_n}, z_{L_n})$, $n = 1, 2, 3, 4$. The spatial separation between the individual and the 4 LEDs can be spoken to as the accompanying equation:

$$L^{(n)} = \sqrt{(x_0 - x_{L_n})^2 + (y_0 - y_{L_n})^2 + (z_0 - z_{L_n})^2} \quad (24)$$

Regarding the construction of the fitness function, the spatial separation deviation is utilized to gauge an individual is near the perfect location or not:

$$fitness\left(x_0, y_0, z_0, d_c^{(1)}, d_c^{(2)}, d_c^{(3)}, d_c^{(4)}\right) = \sqrt{\sum_{i=1}^{4}(L^{(i)} - d_c^{(i)})^2} \quad (25)$$

In the event that the individual is sufficiently close to the perfect location, the estimation of the fitness function ought to be near zero.

3.4.3 Selection Operation

With a specific end goal to choose the amazing individual, the roulette technique is presented. In this scene, lower fitness esteem implies a superior solution. The person with lower fitness esteem ought to be chosen with a higher likelihood. Expect the fitness lattice $\vec{F}$ contains the fitness estimation of all people:

$$\vec{F} = \{F_1, F_2, \ldots F_m\} \quad (26)$$

The chose likelihood of the kth individual is [23]:

$$P_k = 1 - \frac{F_k}{\sum_{i=1}^{m} F_i} \quad (27)$$

3.4.4 Crossover Operation

With a specific end goal to keep up the assorted variety of the types of GA, before playing out the crossover operation, a likeness check ought to be performed ahead of time. The particular operation is as per the following: (1) Select two people randomly, calculate the likeness constant of the two individual by Eq. (17); (2) If the similitude constant is higher than the limit, this crossover operation is invalid and ought to be executed again.

3.4.5 Mutation Operation

The change operation of the traditional GA is turn over the estimation of a bit, the operand only incorporates one quality which can't ensure the allelic assorted variety. And this is additionally the reason for the untimely occurrence in GA. To improve the positioning precision and increase speed the convergence rate, another change administrator is presented. Here, two chromosomes from two people partake the mutation operation. Comprehensive or rationale operation and restrictive or rationale operation is done on the two chromosome fragments separately. Expect the two chromosome fragments from two people are $\oplus$ and $\odot$, the two chromosome fragments after mutation operation $\oplus$ and $\odot$ can be composed as the accompanying equation:

$$\acute{l_1} = l_1 \oplus l_2 \quad (28)$$

$$\acute{l_1} = l_1 \odot l_2 \quad (29)$$

where $\oplus$ and $\odot$ speak to the XOR and XNOR operation individually.

After the mutation operation, the intelligent relationship on allelic focuses ought to be reciprocal which stays away from the missing qualities phenomenon in the population.

3.4.6 Algorithm Termination Condition

Typically, the specific upgraded exactness σ is utilized as the termination condition in GA. Albeit a few strategies depicted above have been connected to keep the untimely phenomenon in GA, now and then because of the absence of hereditary assorted variety, the calculation result can't converge to the ideal solution after numerous generations. So keeping in mind the end goal to take out this condition, most extreme iterations number n_{max} ought to be given. In the event that the generation is in overabundance of n_{max}. The positioning algorithm ought to be keep running from the earliest starting point.

IV. EXPERIMENTAL SETTINGS AND SIMULATION RESULTS

AKFTDP is proposed for RFID-based positioning system. In the simulation scenario, the kind RFID reader used is a Laird-S8658WPL UHF RFID System which will in MHz unit. The main working frequency is 965 MHz, the power is 10 W and the gain is 6dBiC. As the AKF performs better, the indoor positioning is tranquil capable of improvement. Table 1.shows the experimental settings.

Table 1. Experimental Settings

RFID Reader Type	Laird-S8658WPL UHF RFID
Working Frequency	965 MHz
Power	10 W
Gain	6dBiC
Unit	MHz

4.1 Reality Value Vs Predictive Value of AKFTDP Vs PSOBP:

Figure 1 and Figure 2 portrays the reality value and the predictive value of the proposed AGA-TDP and PSO-BP. From the results it is evident that the proposed AGA - TDP is very closer to the reality value when compared with the existing PSO-BP. The result values are given in Table 2.

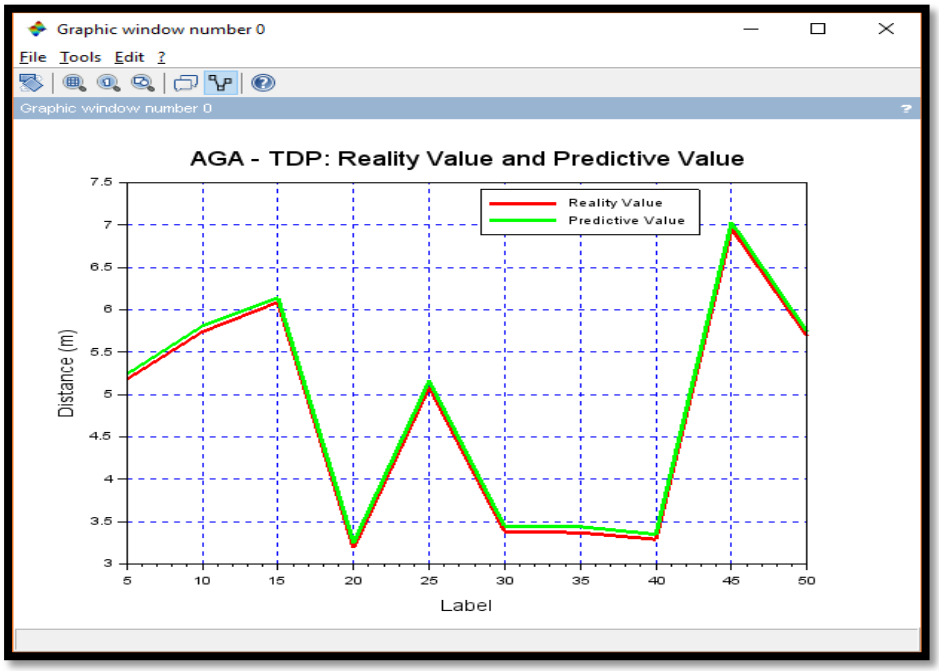

Figure 1. AGA-TDP: Reality Value and Predictive Value

Figure 2. PSO - BP: Reality Value and Predictive Value

Table 2. Performance Analysis: Reality Value Vs Predictive Value

Labels	Reality Value	AGA-TDP	PSO-BP
5	5.18	5.24	5.44
10	5.74	5.81	6.00
15	6.09	6.14	6.37
20	3.19	3.25	3.42
25	5.09	5.16	5.35
30	3.38	3.44	3.61
35	3.37	3.44	3.64
40	3.29	3.35	3.53
45	6.96	7.03	7.22
50	5.69	5.74	5.98

4.2 Error Rate AKFNLA Vs PSO BP:

Error Rate is defined as the measure of effectiveness of the system. It can also be said as the ratio of the number of errors that araised to the total number of units.

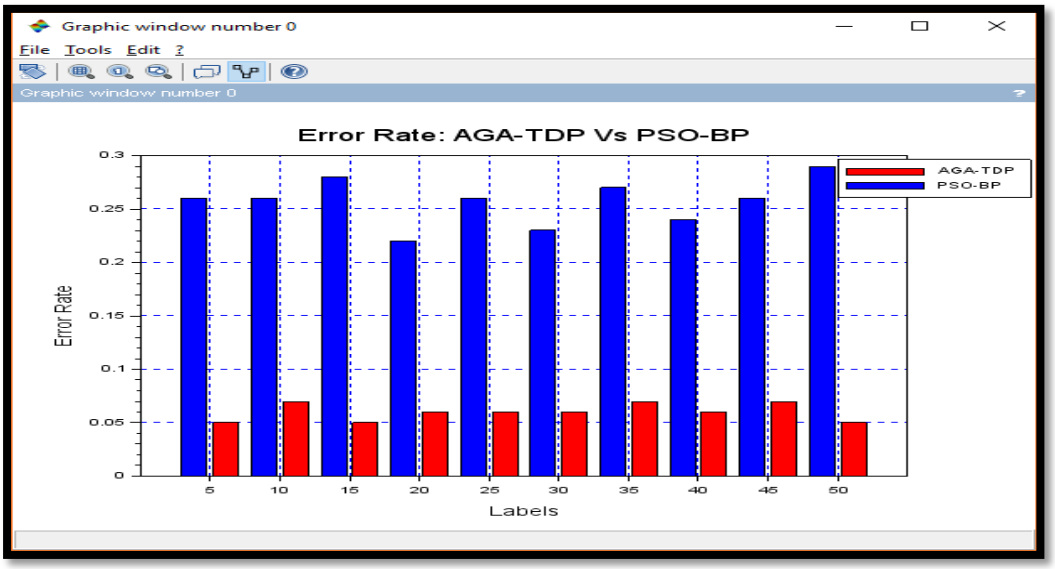

Figure 3. Error Rate: AKF NLA Vs PSO BP

Table 3. Performance Analysis: Error Rate

Labels	AGA-TDP	PSO-BP
5	0.05	0.26
10	0.07	0.26
15	0.05	0.28
20	0.06	0.22
25	0.06	0.26
30	0.06	0.23
35	0.07	0.27
40	0.06	0.24
45	0.07	0.26
50	0.05	0.29

4.3 Convergence Speed

Convergence is the combination of more than one technologies in a single device or system, where convergence speed of the network reflects the performance of the algorithm.

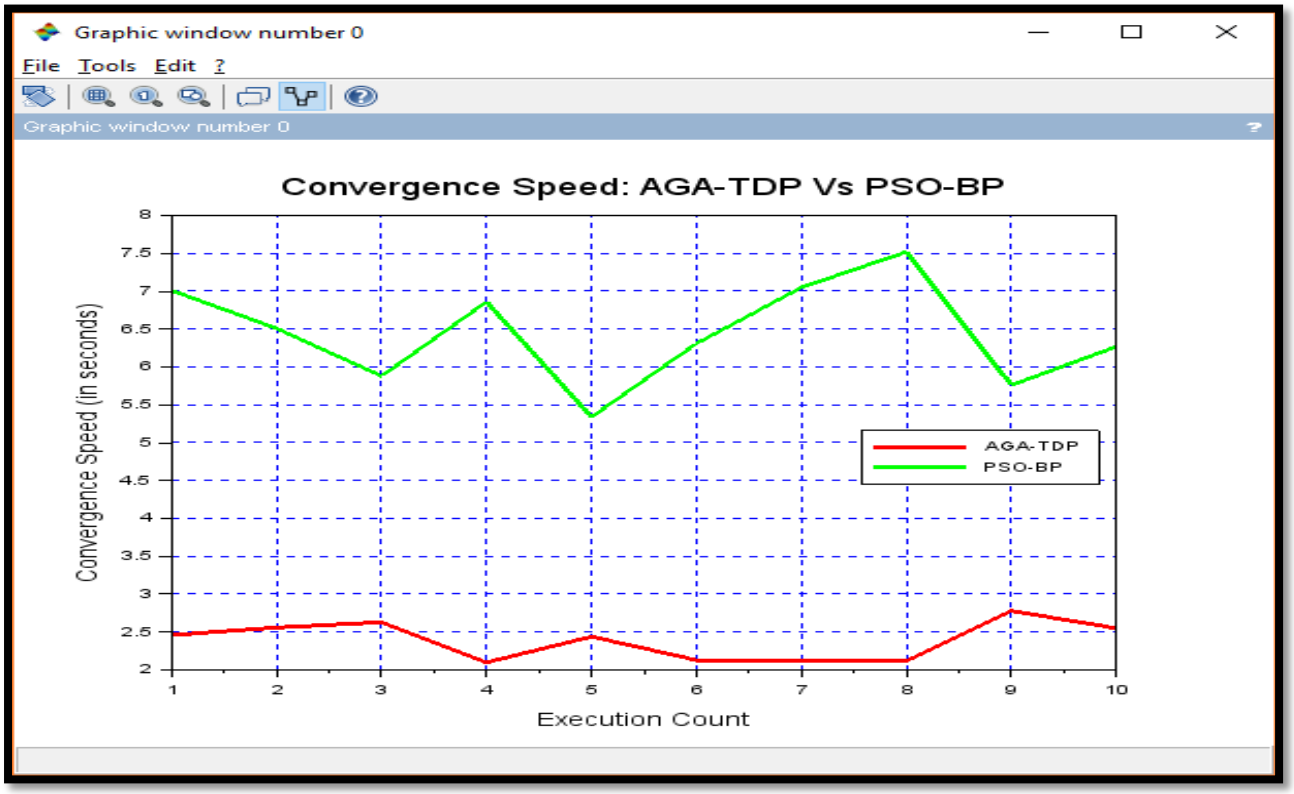

Figure 4. Convergence Speed: AGA-TDP

Table 4. Convergence Speed

Execution	AGA-TDP	PSO-BP
1	2.46	7.01
2	2.56	6.51
3	2.63	5.88
4	2.10	6.86
5	2.44	5.34
6	2.13	6.31
7	2.13	7.05
8	2.12	7.52
9	2.78	5.76
10	2.55	6.27

4.4 Accuracy

Accuracy is a measure of a value which denotes how close a result comes to the true value.

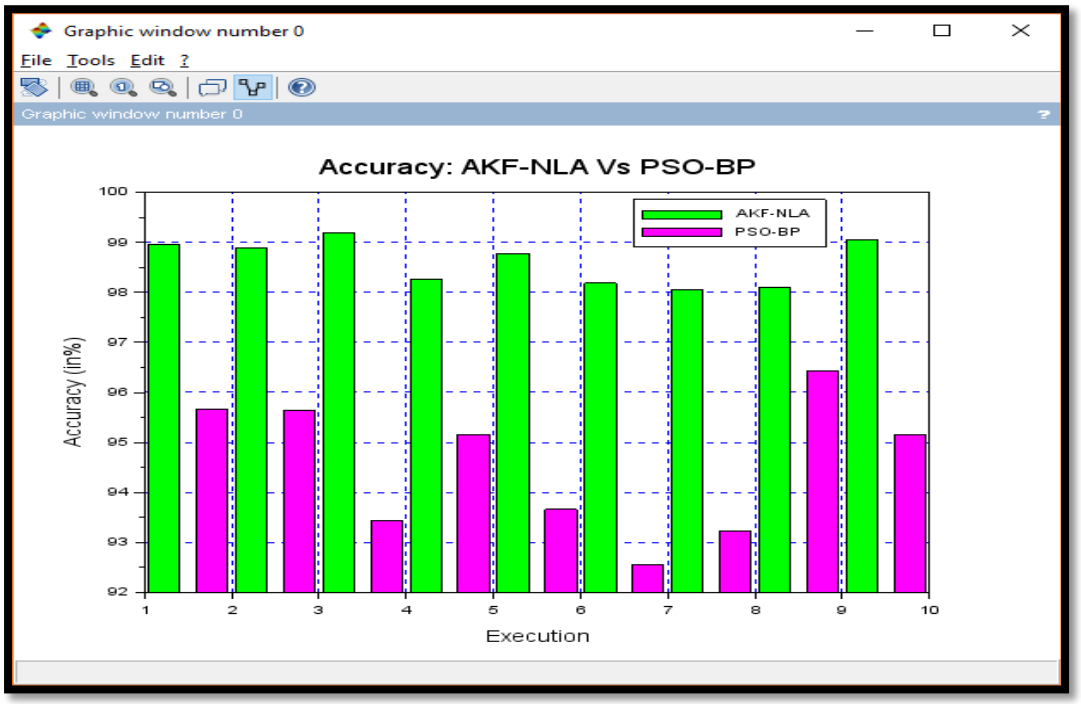

Figure 5. Accuracy: AGA-TDP

Table 5. Accuracy

Execution	AGA-TDP	PSO-BP
1	98.96	95.23
2	98.88	95.67
3	99.19	95.65
4	98.26	93.44
5	98.77	95.16
6	98.18	93.66
7	98.05	92.56
8	98.10	93.24
9	99.04	96.42
10	99.11	95.16

V. CONCLUSION

Visible light communication (VLC) based indoor 3D positioning is gaining its interest in RFID communication. This happened due to lessening features from various light emitting diodes (LEDs), the three-dimensional directions of the receiver possibly will perform constraint equations. In certain areas of VLC positioning system, positioning precision is constrained due to the system noise and non-perfect gadgets. In this research work, an adaptive GA is used to subtle the positioning errors that facilitate 3D of the receiver. Positioning directions are managed by evaluated as indicated by the principle of trilateration.Performance metrics such as reality value versus predictive value, error rate, convergence speed and accuracy are taken into account for comparing the proposed work with the existing work PSO-BP. Results demonstrated that the proposed AGA-TDP performs better than that of PSO-BP.

VI. REFERENCES

[1]. Z. Yang, Z. Zhou, Y. Liu, Fromrssi to csi: Indoor localization via channel response, ACM Computing Survey 46 2) 2013) 25:1–25:32.

[2]. C. Luo, H. Hong, L. Cheng, M. C. Chan, J. Li, Z. Ming, Accuracy-aware wireless indoor localization: Feasibility and applications, Journal of Network and Computer Applications 62 2016) 128–136.

[3]. M. Youssef, M. Mah, A. Agrawala, Challenges: Device-free passive localization for wireless environments, in: Proceedings of the 13th Annual ACM International Conference on Mobile Computing and Networking MobiCom 2007), 2007, pp. 222–229.

[4]. L. Ni, Y. Liu, Y. C. Lau, A. Patil, LANDMARC: indoor location sensing using active rfid, in: Proceedings of the First IEEE International Conference on Pervasive Computing and Communications PerCom 2003), 2003, pp. 407–415.

[5]. C. Wu, Z. Yang, Y. Liu, W. Xi, WILL: Wireless indoor localization without site survey, in: Proceedings of the 31st IEEE International Conference on Computer Communications INFOCOM 2012), 2012, pp. 64–72.

[6]. L. Yang, Y. Chen, X.-Y. Li, C. Xiao, M. Li, Y. Liu, Tagoram: Real-time tracking of mobile rfid tags to high precision using cots devices, in: Proceedings of the 20th Annual International Conference on Mobile Computing and Networking MobiCom 2014), 2014, pp. 237–248.

[7]. T. Liu, Y. Liu, L. Yang, Y. Guo, W. Cheng, Backpos: High accuracy backscatter positioning system, IEEE Transactions on Mobile Computing PP 99) 2015) 1–1.

[8]. Z. Yang, C. Wu, Z. Zhou, X. Zhang, X. Wang, Y. Liu, Mobility increases localizability: A survey on wireless indoor localization using inertial sensors, ACM Computing Survey 47 3) 2015) 54:1–54:34.

[9]. C. Xu, B. Firner, R. S. Moore, Y. Zhang,W. Trappe, R. Howard, F. Zhang, N. An, SCPL: Indoor Device-free Multi-subject Counting and Localization Using Radio Signal Strength, in: Proceedings of the 12th International Conference on Information Processing in Sensor Networks IPSN 2013), 2013, pp. 79–90.

[10]. D. Zhang, J. Zhou, M. Guo, J. Cao, T. Li, Tasa: Tag-free activity sensing using rfid tag arrays, IEEE Transactions on Parallel and Distributed Systems 22 4) 2011) 558–570.

[11]. Y. Liu, Y. Zhao, L. Chen, J. Pei, J. Han, Mining frequent trajectory patterns for activity monitoring using radio frequency tag arrays, IEEE Transactions on Parallel and Distributed Systems 23 11) 2012) 2138–2149.

[12]. W. Ruan, L. Yao, Q. Z. Sheng, N. Falkner, X. Li, T. Gu, Tagfall: Towards unobstructive fine-grained fall detection based on uhf passive rfid tags, in: Proceedings of the 12th International Conference on Mobile and Ubiquitous Systems: Computing, Networking and Services, 2015, pp. 140–149.

[13]. M. Breitenstein, F. Reichlin, B. Leibe, E. Koller-Meier, L. Van Gool, Online multiperson tracking-by-detection from a single, uncalibrated camera, IEEE Transactions on Pattern Analysis and Machine Intelligence 33 9) 2011) 1820–1833.

[14]. H. Dai, Z.-M. Zhu, X.-F.Gu, Multi-target indoor localization and tracking on video monitoring system in a wireless sensor network, Journal of Network and Computer Applications 36 1) 2013) 228–234.

[15]. B. Yang, Y. Lei, B. Yan, Distributed multi-human location algorithm using naive bayes classifier for a binary pyroelectric infrared sensor tracking system, IEEE Sensors Journal PP 99) 2015) 1–1.

[16]. T. Helten, M. Muller, H.-P. Seidel, C. Theobalt, Real-time body tracking with one depth camera

and inertial sensors, in: Proceedings of IEEE International Conference on Computer Vision ICCV 2013), 2013, pp.1105–1112.

[17]. J. Wilson, N. Patwari, Radio tomographic imaging with wireless networks, IEEE Transactions on Mobile Computing 9 5) 2010) 621–632.

[18]. A. Saeed, A. Kosba, M. Youssef, Ichnaea: A low-overhead robust wlan device-free passive localization system, IEEE Journal of selected Topics in Signal Processing 8 1) 2014) 5–15.

[19]. K. Wu, J. Xiao, Y. Yi, D. Chen, X. Luo, L. Ni, Csi-based indoor localization, IEEE Transactions on Parallel and Distributed Systems 24 7) 2013) 1300–1309.

[20]. C.Wu, Z. Yang, Z. Zhou, X. Liu, Y. Liu, J. Cao, Non-invasive detection of moving and stationary human with wifi, IEEE Journal on Selected Areas in Communications 33 11) 2015) 2329–2342.

[21]. F. Adib, Z. Kabelac, D. Katabi, Multi-person localization via rf body reflections, in: Proceedings of the 12th USENIX Conference on Networked Systems Design and Implementation NSDI 2015), 2015, pp. 279–292.

[22]. Changzhi Wang, Fei Wu, Zhicai Shi, Dongsong Zhang, Indoor positioning technique by combining RFID and particle swarm optimization-based back propagation neural network, Optik - International Journal for Light and Electron Optics, Volume 127, Issue 17, 2016, pp 6839-6849.